Surface chemistry, charge and ligand type impact the toxicity of gold nanoparticles to *Daphnia magna*†

Jared S. Bozich,[a] Samuel E. Lohse,[b] Marco D. Torelli,[c] Catherine J. Murphy,[b] Robert J. Hamers[c] and Rebecca D. Klaper*[a]

Nanoparticles (NPs) are the basis of a range of emerging technologies used for a variety of industrial, biomedical, and environmental applications. As manufactured NP production increases, so too does the concern about their release into the environment and potentially harmful effects. Creating nanomaterials that have minimal negative environmental impact will heavily influence the sustainability of nanomaterials as a technology. In order to create such NPs, the mechanisms that govern NP toxicity need to be better elucidated. One aspect of NP structure that may influence toxicity is the identity and charge of ligand molecules used to functionalize the NP surface. These surface chemistries have the potential to increase or decrease negative biological impacts, yet their impacts are poorly understood. In this study, the toxicity of three types of functionalized ~4–5 nm gold NPs (AuNPs), polyallylamine hydrochloride (PAH–AuNPs), citrate (Cit–AuNPs) and mercaptopropionic acid (MPA–AuNPs) as well as cetyltrimethylammonium bromide-functionalized gold nanorods (CTAB–AuNRs) were evaluated in the toxicological model species, *Daphnia magna*. In order to get the most detailed information on NP toxicity in *D. magna*, both acute and chronic toxicity assays were performed. Acute exposure toxicity assays show that overall the negatively-charged AuNPs tested are orders of magnitude less toxic than the positively-charged AuNPs. However, chronic exposure assays show that both positively and negatively-charged particles impact reproduction but potentially through different mechanisms and dependent upon functional group. In addition, while select ligands used in NP functionalization (such as CTAB) that are toxic on their own can contribute to observed NP toxicity, our acute toxicity assays indicate that minimally toxic ligands (such as PAH) can also cause significant toxicity when conjugated to NPs. This research demonstrates that surface chemistry plays a pivotal role in NP toxicity and that surface chemistry has the potential to affect the sustainability of these materials.

Nano impact

Understanding the impacts of engineered NP exposure on aquatic organisms is essential to predict the environmental implications of nanotechnology, however issues with nanomaterial synthesis and characterization often plague these studies. In this study the acute and chronic toxicity of well characterized gold nanoparticles functionalized with ligands of differing charges were investigated in *Daphnia magna*. We found that AuNP toxicity was highly dependent on both NP charge and ligand identity where positively charged nanomaterials were more toxic and certain ligands were only toxic when associated with the nanomaterial. Select negatively charged nanomaterials also impacted reproduction. This experiment illustrates the need for well-characterized nanomaterials to determine the impacts of nanomaterial properties on toxicity to inform the safe and sustainable development of nanomaterials.

[a] *School of Freshwater Sciences, University of Wisconsin Milwaukee, 600 E. Greenfield Ave, Milwaukee, WI 53204, USA. E-mail: rklaper@uwm.edu; Fax: +414 382 1705; Tel: +414 382 1713*
[b] *Department of Chemistry, University of Illinois at Urbana-Champaign, 600 S. Mathews Ave, Urbana, IL 61801, USA*
[c] *Department of Chemistry, University of Wisconsin-Madison, 1101 University Ave, Madison, WI 53706, USA*
† Electronic supplementary information (ESI) available. See DOI: 10.1039/c4en00006d

Introduction

In the U.S. alone, the engineered nanoparticle (NP) industry is a multibillion-dollar industry and is predicted to increase to a one-trillion-dollar industry by 2015.[1] One study estimates that 63–91% of over 260 000–309 000 metric tons of the world NP production in 2010 entered our environment through landfills.[2] As production increases, there is a concern about

260 | *Environ. Sci.: Nano*, 2014, **1**, 260–270

This journal is © The Royal Society of Chemistry 2014

the potential environmental and health effects of NP exposures. The surfaces of NPs are typically modified with surface functional groups that control properties such as NP stability.[3–5] To create NPs that are less toxic and more environmentally sustainable there is a need to understand which NPs may cause harm to the environment and what physiochemical properties determine their impacts on organisms. This involves: 1) understanding the interaction of NPs with an organism; 2) which physiochemical properties of a NP best predict toxicity; and 3) how alterations in NP surface chemistry can alleviate toxic impacts. To better understand these factors, experiments are needed that use fine-scale alterations in NP surface chemistry to probe the interactions of NPs with cells, tissues and organisms. In addition, it is necessary to create NPs that have specific and well-defined bulk and surface chemistries to determine how their chemical composition and structure of the NP and surface functional groups may influence toxicity.

Although many studies on toxicity of NPs have been conducted to date, the mechanisms that govern NP toxicity are still in question as experimental artifacts and the design of experiments can impede understanding of the fine scale interactions of NPs with biological entities.[6] For example, the charge of the NP surface has been implicated as a major factor in toxicity.[7–12] Yet the initial charge of a particle may be altered during an experiment due to interactions with media.[13–16] Particle size and surface chemistry have also been suggested to impact NP toxicity[17–23] as both particle size and surface chemistry can influence particle uptake and partitioning in organelles and tissues.[24–29] The density of ligands on the NP surface is often poorly characterized, however it may also have an impact on toxicity.[30,31] Aggregation over time in experimental media or in the environment, can either increase or decrease NP toxicity and may have a significant impact on toxicity.[32–34] Byproducts from particle synthesis or the ligands alone may cause toxicity.[35] Few studies attempt to include controls for several of these factors, which can complicate conclusions of properties associated with toxicity. Finally, many studies that have been conducted to date have been carried out using *in vitro* systems and only over short time periods, which may not accurately reflect real world whole organismal interactions with NPs.[8,36,37]

To examine the specific interactions of NPs with differing surface functionalization in a whole organism model, we evaluated the *in vivo* toxicity of a library of well-characterized gold NPs (AuNPs) with differing surface functionalities to the aquatic toxicity model *Daphnia magna*. AuNPs were chosen as a model NP as they can be synthesized with very fine control of size and shape, are readily altered with well-know surface chemistries, have a low environmental background level (so they can be easily tracked within an organism), and have many potential commercial applications due to their unique optical properties and their benign nature. Furthermore, unlike other functionalized metal and metal oxide NPs, AuNPs are resistant to dissolution or significant changes in size or shape under typical environmental and biological conditions.[38–41] Applications where these particles have been used range from

cellular imaging,[42] bio-chemical sensing,[43] drug and gene delivery,[44,45] to medical therapeutics.[46] The successful implementation of AuNPs in these applications depend strongly upon appropriate particle functionalization.[47]

In this study, acute and chronic assays were carried out in order to measure both short term and full life cycle effects of various functionalized AuNPs on *Daphnia magna*. Particles were characterized after synthesis and within exposure media to better untangle the biological effects caused by particle stability and aggregation. Controls were designed to take into account the toxicity and other adverse impacts due to free ligands, supernatants containing reagents and NP synthesis byproducts and impurities in reagents. This study begins to address the molecular properties of NPs that influence their toxicity and interactions with aquatic organisms.

Materials and methods

Nanoparticle synthesis and functionalization

All materials were used as received, unless otherwise noted. Gold tetrachloroaurate trihydrate ($HAuCl_4 \cdot 3H_2O$), 3-mercaptopropionic acid (MPA), sodium borohydride ($NaBH_4$), polyallylamine hydrochloride (PAH; M_w 15 000 g mol^{-1}), and silver nitrate ($AgNO_3$) were obtained from Sigma Aldrich. Hexadecyltrimethyl ammonium bromide (CTAB), L-ascorbic acid, and trisodium citrate were obtained from Sigma. Deionized water was prepared using a Barnstead NANOPURE water filtration system. PALL Minimate tangential flow filtration capsules for AuNP purification, with 50 kD pore size was obtained from VWR. TEM grids, SiO on copper mesh (PELCO) were used for transmission electron microscopy studies. Functionalized AuNPs were synthesized using previously reported methods in a millifluidic reactor, which enabled high-throughput NP synthesis. The millifluidic reactor for NP synthesis was assembled (as previously described) from commercially available components: a peristaltic pump (Cole-Palmer Masterflex L/S), Tygon polyvinyl tubing (ID = 2.79 mm), polyethylene Y-mixers (ID = 1.79 mm), and polyethylene joints.[48] AuNPs were synthesized in the reactor at an overall flow rate of 50.0 mL min^{-1}, and experienced a residence time of 3.0 min for the spherical AuNP syntheses, and 20.0 min for the gold nanorod synthesis.

NPs stabilized with four different surface chemistries were synthesized: (1) citrate-functionalized NPs ("Cit–AuNPs"), (2) poly(allylamine) hydrochloride ("PAH–AuNPs"), (3) mercaptopropionic acid-functionalized NPs ("MPA–NPs") and (4) cetyl trimethylammonium bromide-functionalized gold nanorods ("CTAB–AuNRs") (Fig. 1).

Cit–AuNPs (5.0 nm). 5.0 nm citrate AuNPs were synthesized using previously reported procedures.[49] In a typical synthesis, 4.0 L of a growth solution, consisting of aqueous gold tetrachloroaurate ($HAuCl_4$, 10.0 mM) and 10.0 mM sodium citrate$_{(aq)}$, as well as a 4.0 L of an aqueous solution of sodium borohydride (5.0 mM) were prepared. The two solutions were flowed together in a millifluidic synthesis reactor at a flow rate of 50.0 mL min^{-1}, and experienced a residence time of

This journal is © The Royal Society of Chemistry 2014

*Environ. Sci.: Nano*, 2014, **1**, 260–270 | **261**
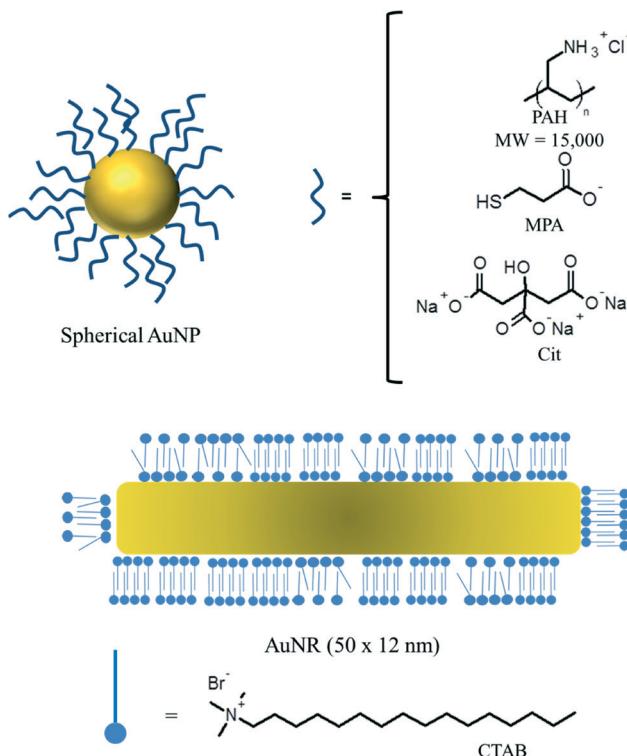
Fig. 1 Schematic representation of functionalized AuNPs used in the toxicology study.

3.0 min. The combined solutions rapidly change color to a deep brown, and then red-brown prior to exiting the reactor. The AuNP solution was collected in an *aqua regia*-cleaned 4.0 L bottles and stirred for 3.0 hours. The Cit–AuNPs were then concentrated and purified by diafiltration (5.0 volume equivalents).[50]

PAH–AuNPs (5.0 nm). Cit–AuNPs were wrapped with polyallylamine hydrochloride (PAH) to prepare 4.0 PAH-functionalized AuNPs, as previously described.[51] Briefly, Cit–AuNPs were dissolved in 20.0 mL of a 1.0 mM aqueous sodium chloride solution to give a final AuNP concentration of approximately 20.0 nM. To each 20.0 mL of polyelectrolyte wrapping solution, 500.0 μL of PAH (10.0 mg mL^{-1}) dissolved in 1.0 mM NaCl was added. The wrapping solution was then mixed at vortex briefly and left to stand for 16 h. The PAH–AuNPs were subsequently purified by centrifugation and washing (55 min at 8000 rcf), in nanopure deionized water. The PAH–AuNPs were then concentrated in a diafiltration membrane.

MPA–AuNPs (4.0 nm). Thiol-stabilized AuNPs were prepared by direct synthesis with sodium borohydride according to previously reported methods.[50,52] Briefly, two 4.0 L aqueous solutions (a growth solution and a reducing agent solution) were prepared. The growth solution contained HAuCl$_4$ (3.0 mM) and MPA (6.0 mM) dissolved in nanopure deionized water. The pH of the growth solution was adjusted to approximately 8.5 by the addition of sodium hydroxide. The other 4.0 L solution consisted of 5.0 mM-aqueous NaBH$_4$. The two

solutions were flowed together in a millifluidic reactor at 50.0 mL min^{-1} and experienced a residence time of 3.0 min. The combined solutions rapidly change color to a deep orange-brown. The AuNP solution was collected in an *aqua regia*-cleaned 4.0 L bottle and stirred for 3.0 hours. The thiol-stabilized AuNPs were then concentrated and purified by diafiltration (40.0 volume equivalents of nanopure deionized water in a 50 kD membrane).

CTAB-stabilized gold nanorods (AuNRs). CTAB-stabilized gold nanorods with aspect ratio (length/width) 4.0 were synthesized using our previously reported seeded growth procedures.[53] Two solutions were prepared: a growth solution and a "Seed" solution. For the growth solution, 10.0 mL HAuCl$_4$ (0.1 M), 16.0 mL AgNO$_3$ (0.01 M), and 11.0 mL of ascorbic acid (0.1 M) were added to 1.0 L of a 0.1 M aqueous CTAB solution. For the seed solution, 2.4 mL of a previously prepared gold NP seed dispersion (aged 2 hours) was added to 998.0 mL of a 0.1 M CTAB solution. The solutions were mixed within the flow reactor (flow rate = 50.0 mL min^{-1}), and the AuNR growth solution experienced a residence time of approximately 15.0 min in the reactor before being deposited into an *aqua regia*-cleaned 4.0 L bottle. AuNRs were purified and concentrated by centrifugation and washing (two times, 20 min at 11 000 rcf) with nanopure deionized water.

Functionalized gold nanoparticle characterization and analysis

Gold NP solutions were analyzed using a combination of UV-vis absorption spectroscopy, transmission electron microscopy (TEM), ζ-potential analysis, Dynamic Light Scattering (DLS) and x-ray photoelectron spectroscopy (XPS). UV-vis absorbance spectroscopy analysis was performed using a Cary 500 Scan UV-vis-NIR Spectrophotometer. For transmission electron microscopy analysis, a small aliquot of the purified AuNP solution was dropcast onto a SiO/Cu mesh/formvar TEM grid (Ted Pella), and examined using a JEOL 2100 Cryo TEM. Size distributions for the AuNPs were determined using ImageJ analysis, according to previously reported procedures.[54] For XPS analysis, purified AuNP solutions were dropcast onto indium foil and analyzed using a custom-designed, ultrahigh vacuum Physical Electronics XPS system with a monochromated Al X-ray source. DLS and ζ-potential (Malvern Instruments, model #ZEN3600) of the functionalized NPs were obtained in both nanopure deionized water ([AuNP] = 10 nM, pH = 5.8) and daphnid media ([AuNP] = 10 nM, pH = 6.8) to determine aggregate sizes and stability of particles in MHRW prior to and during the experiment.

Ligand densities for particles at the beginning of the experiment were determined using XPS. Detailed procedures for XPS sample preparation and analysis are presented in the ESI.† Briefly, NP solutions were dripped onto Si wafers, and XPS features characteristic for each molecule were measured and normalized against gold as an internal standard. A quantitative numerical modeling procedure was validated and used to correct for NP curvature and scattering effects. These measurements are presented in Table 3.

262 | *Environ. Sci.: Nano*, 2014, **1**, 260–270

This journal is © The Royal Society of Chemistry 2014

Daphnia magna toxicity assays

Daphnia magna are freshwater invertebrates that selectively filter feed in both benthic and pelagic regions of the aquatic environment. Important to aquatic food webs and designated by the U.S. Environmental Protection Agency (U.S. EPA) as a model organism, *Daphnia magna* are widely accepted as a model organism for assessing the toxicity of environmental contaminates and experience reduced reproduction, growth and increased mortality with exposure to toxic substances or substandard food items.[55]

Daphnids were bred in the Klaper lab at UWM-School of Freshwater Sciences and cultures were maintained in tanks of moderately hard reconstituted water (MHRW) at 20 °C on a 16:8 light/dark cycle (per OECD and EPA protocols).[56,57] Daphnids were fed a diet composed of freshwater algae (*Selenastrum capricornutum*) with an algal density of 400 000 algal cells mL^{-1} and the supernatant of 405 mg of alfalfa (*Medicago sativa*) suspended in 50 mL ultrapure water after 20 min of stirring and 10 min of settling.

D. magna were exposed to concentrations of four types of functionalized AuNPs, described above, over a concentration range of 0.001–25 mg L^{-1} (see particle descriptions, and synthesis methods). In addition, the corresponding ligands (Cit, MPA, PAH and CTAB) were tested at 0.001–25 mg L^{-1}. These concentrations were chosen to be far in excess of the total ligand present in the NP suspension. The supernatants and filtrates were collected from the particle purification process and then the supernatant and filtrate stocks were diluted to a concentration of 0.001–25 mg L^{-1} (based on the estimated total ligand concentration in the supernatant). AuNP stock solutions were prepared at a maximum concentration of 2000 mg L^{-1}.[58,59] Accordingly, daphnids were exposed to functionalized AuNPs at a maximum concentration of 25 mg L^{-1} in the acute and chronic exposure studies.

For 48 hour acute studies five female daphnid neonates less than 48 hours old were placed in 100 mL of MHRW (control) or NPs in MHRW (experimental) totaling 100 mL in volume. A minimum of three replicates was carried out for each concentration and the mortality of daphnids were assessed per beaker by calculating the remaining percentage of daphnids alive.

For chronic exposures, daphnids less than 48 hours old were exposed to NPs for 21 days below the concentrations that were found to be acutely toxic. Five neonates were placed in 94 mL of MHRW (control) or NPs in a static renewal exposure where 100% media exchange occurred three times per week. *Daphnia magna* were fed 4 mL of algae (*Selenastrum capricornutum*) and 2 mL of alfalfa (*Medicago sativa*) at each exchange period to bring the total beaker volume to 100 mL. Mortality and reproduction were measured during the media changes and daphnid size was measured at the end of the exposure. Size was measured on day 21 of the exposure as the length of the daphnid from the top of the helmet to the base of the spine.

Exposures adhered to the mortality and reproduction guide lines designated by the OECD guidelines for the Testing of Chemicals.[60] Alterations were done to the exposures to account for discrepancy introduced by changes in population density through the exposure.[23] Daphnids were held at a concentration of one daphnid per 20 mL of media. Reproduction was calculated for the number of remaining individuals at the time of measurement and stated as the mean number of neonates generated per remaining individual.

ICP-MS determination of AuNP uptake by *Daphnia magna*

In order to determine how the surface chemistry of the AuNPs influenced NP uptake by daphnids as well as the external adsorption onto the daphnid carapace, gold content both inside and outside of the daphnids were quantified by ICP-MS analysis. For the ICP studies, *D. magna* were exposed to AuNPs at a concentration of 5.0 ppb for a period of 6 h, under the standard acute toxicity conditions. After 6 h, five daphnids were removed from each of the AuNP-containing media and either treated with or without a 100 mM iodide etchant solution for 5 min to differentiate the particles adsorbed onto the daphnid carapace *vs.* particles ingested. Daphnids were then individually digested in 1.0 mL of freshly prepared *aqua regia* for 2 h. Afterwards, the digest solutions were diluted to a final volume of 10.0 mL with nanopure water. The digested *Daphnia magna* samples were analyzed by ICP-MS (Perkin-Elmer SCIEX Elan DRCe) to determine the total gold concentration. The total Au concentration was then converted to the number of AuNPs taken up/adsorbed by each daphnid using the density of bulk gold and the volume of each AuNP in order to determine the number of Au atoms per NP.

Statistical analysis

D. magna body size and reproduction were normalized to control averages to account for changes in daphnid populations over time. Some of the data failed to meet the assumptions of normality for the independent *t* test analysis. Therefore, the effects of NP exposures on daphnid fecundity, mortality and body size were weighed against controls by the nonparametric Mann–Whitney *U* test for two-independent samples. Values were considered significant at $p < 0.05$. SPSS (IBM 2013) was the program chosen to carry out statistical analysis.

Gold NP uptake in *D. magna* (see ESI† Fig. S6) was analyzed using the independent *t* test in Microsoft Excel 2013. Values were considered significant at $p < 0.05$.

Results

Gold nanoparticle characterization

AuNPs were characterized using TEM, UV-vis absorbance spectroscopy, and dynamic light scattering in order to rigorously determine AuNP size. The size and surface chemistry characterization data for the AuNPs is presented in detail in Table 1. Representative TEM images and size analysis for the spherical AuNPs are provided in the ESI† (Fig. S1 and S2, respectively). The CTAB-stabilized AuNRs had a longitudinal diameter of ~50 nm, and a transverse diameter of ~12 nm. PAH–AuNPs had a mean diameter of 4.7 ± 1.4 nm (1σ). Cit–AuNPs had a mean core diameter of 4.9 ± 1.4 nm. MPA–AuNPs had a mean core diameter of 3.8 ± 1.1 nm. Here, the polydispersity in the

This journal is © The Royal Society of Chemistry 2014

Environ. Sci.: Nano, 2014, **1**, 260–270 | 263

Table 1 AuNP characterization as synthesized

AuNP sample	SPR λ_{max} (nm)	d_{core} (nm)	D_h (nm)	ζ-potential (mV)
CTAB–AuNRs	512 778	50 × 14	20.7 ± 0.5	16.7 ± 1.5
PAH–AuNPs	524	4.7 ± 1.2	17.9 ± 0.9	17.9 ± 0.9
Cit–AuNPs	518	4.9 ± 1.4	12.8 ± 1.2	−15.3 ± 1.5
MPA–AuNPs	512	3.8 ± 1.1	8.0 ± 1.2	−18.5 ± 1.3

Table 3 AuNP ligand density determined by XPS

AuNP sample	Measured density
CTAB–AuNR	7.6×10^{14} and 1.39×10^{15} molecules cm^{-2}
PAH–AuNP	1.12×10^{15} formula units cm^{-2}
Cit–AuNP	4.7×10^{14} molecules cm^{-2}
MPA–AuNP	5.6×10^{14} molecules cm^{-2}

sample is given as a single standard deviation from the mean core diameter. The surface charge of the AuNPs was determined using ζ-potential analysis (Table 1).

The ligand density of the AuNP library was determined using XPS and with the exception of CTAB–AuNR Table 3 shows that the ligand densities for Cit–AuNP and MPA–AuNP are nearly the same and are also nearly identical to values previously reported for densely-packed self-assembled mono-layers on planar gold surfaces.[61] Because CTAB–AuNR is a rod shaped particle, a max/min range based on the assumption of a planar and spherical particle has been provided. As the rods still possess a significant amount of curvature the ligand density should be closer to the lower density estimate. Though there are physically more CTAB molecules, CTAB coats the AuNR in a bilayer.[62,63] Thus, the increased number of CTAB ligands is not due to a higher packing density. The number of ligands on the outer leaflet of CTAB–AuNR is comparable to the other functionalized particles in this study. For PAH–AuNP, the polymeric nature of the PAH ligand makes it difficult to determine an equivalent molecular density.

Stability of AuNPs in daphnid media

In order to better connect the physiochemical properties of the AuNPs tested with their acute mortality in *Daphnia magna*, we monitored the changes in the AuNP physiochemical properties the AuNPs undergo following dispersion in daphnid media using UV-vis absorption spectroscopy, DLS, and ζ-potential analysis. The positively-charged AuNPs (the CTAB–AuNRs and the PAH–AuNPs) showed no evidence of changes in size, shape, or aggregation state (based on their UV-vis spectra, Fig. S3,† and DLS analysis, Table 2). In contrast, the negatively-charged AuNPs show evidence of aggregation following dispersion in daphnid media. This aggregation is evidenced by broadening of the Surface Plasmon Resonance (SPR) absorbance (~520 nm) in the UV-vis spectra, and a significant increase in their hydrodynamic diameter over the course of the 48 h exposure time (D_h, see Table 2). Interestingly, the

Table 2 AuNP characterization in daphnid media

AuNP sample	Time (h)	D_h (nm)	Z-potential (mV)
CTAB–AuNRs	0	16.6 ± 2.0	28.1 ± 1.6
CTAB–AuNRs	48	17.5 ± 0.2	27.7 ± 1.8
PAH–AuNPs	0	52.8 ± 1.7	11.8 ± 5.2
PAH–AuNPs	48	55.9 ± 4.1	20.4 ± 0.4
Cit–AuNPs	0	21.9 ± 0.9	−15.3 ± 1.5
Cit–AuNPs	48	90.8 ± 5.9	−5.6 ± 0.2
MPA–AuNPs	0	50.7 ± 1.1	−9.1 ± 5.3
MPA–AuNPs	48	750.6 ± 8.2	−11.0 ± 1.0

structure of the aggregated Cit–AuNPs appears to be different from the MPA–AuNP aggregates. TEM analysis of the AuNP aggregates shows significant fusion of the Cit–AuNP cores to form larger AuNPs and wire-like structures after 48 h, while the MPA–AuNP aggregates appear to consist primarily of large, loosely bound networks of AuNPs with an ~4 nm primary particle size (Fig. 2). The MPA–AuNPs could be re-suspended from their aggregated state by gentle agitation, while the Cit–AuNPs could not, which would be consistent with the structure of the aggregates observed in the TEM images (Fig. S5†).

Effects of AuNPs on daphnid acute mortality

Particle surface chemistry and stability played an important role in daphnid survival, with positively-charged particles, CTAB–AuNRs and PAH–AuNPs, being orders of magnitude more toxic than the negatively-charged particles, Cit–AuNPs and MPA–AuNPs. CTAB and PAH–AuNPs significantly affected daphnid mortality (93% mortality, $U = 0$, $p < 0.05$; and 40% mortality, $U = 0$, $p < 0.05$, respectively) at concentrations as low as 10 μg L^{-1} (Fig. 3). However, PAH and CTAB–AuNPs demonstrated similar toxicity at 5 μg L^{-1}, showing 13% mortality. Cit and MPA–AuNPs did not significantly affect *Daphnia magna* mortality at all concentrations tested ($p > 0.05$), which reached an order of magnitude higher than the positively charged particle. Positively-charged particles were also more stable in the MHRW media (Table 2).

Of the four ligands tested, CTAB was the only ligand that by itself significantly affected *D. magna* mortality compared to control daphnids (Fig. 3). CTAB ligand caused the same daphnid mortality as CTAB–AuNR acute exposure, causing 13% mortality at 5 μg L^{-1}, 93% mortality at 10 μg L^{-1} and 100% mortality at 50 μg L^{-1} (Fig. 3). The PAH ligand, unlike the PAH–AuNP, did not affect daphnid mortality at the concentrations that were significantly impacting daphnid mortality in the PAH–AuNP acute assay (Fig. 3). Citrate and MPA free ligands, like Cit and MPA–AuNPs, had no impact on daphnid mortality.

When comparing toxicity to that of supernatants and filtrates (collected from the particle purification process), only the supernatants significantly impacted daphnid survival with PAH–AuNP supernatant being the more toxic of the two positively-charged supernatants (Fig. 2). PAH–AuNP supernatant significantly affected daphnid mortality up to 5 μg L^{-1} causing 73% mortality ($U = 0$, $p < 0.05$) and 100% mortality at 10 and 50 μg L^{-1} ($U = 0$, $p < 0.05$). UV-vis and TEM analysis of the PAH–AuNP supernatant indicated that, unlike the other supernatants tested in this study, the PAH–AuNP

264 | *Environ. Sci.: Nano*, 2014, **1**, 260–270

This journal is © The Royal Society of Chemistry 2014
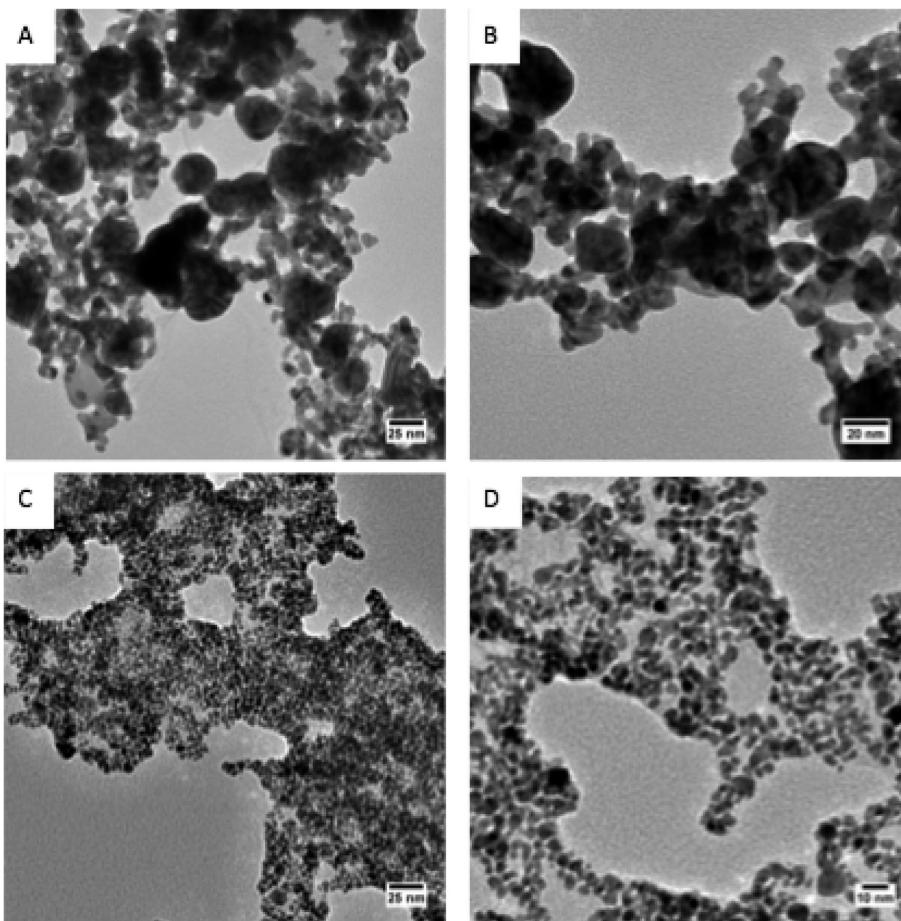
Fig. 2 Agglomerated *vs.* aggregated AuNPs. TEM images of 4.0 nm Cit–AuNPs (A, B) and MPA–AuNPs (C, D) immersed in daphnid media for 48 h. Close examination of the aggregated Cit–AuNPs reveal that the AuNPs have formed extended networks of irregular nanowires and large particles. In contrast, the MPA–AuNPs remain dispersed, but closely associated individual AuNPs. Scale bar in (A) and (C) is 25 nm. Scale bar in (B) is 20 nm. Scale bar in (D) is 10 nm.
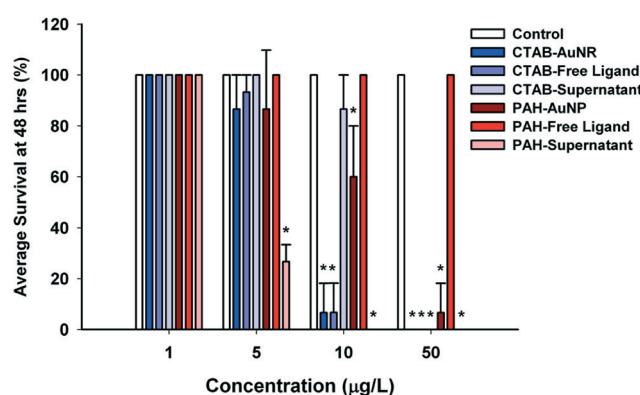
Fig. 3 Effects of AuNPs, free ligands and impurities on daphnid acute mortality. Effects of AuNP exposure on daphnid mortality after 48 hour exposure to 1, 5, 10 and 50 μg L^{-1} CTAB or PAH–AuNPs, free ligands and supernatants. Acute mortality evaluated by Mann–Whitney U test for two independent samples. Asterix indicate significant difference from control ($p < 0.05$).

supernatant contained a low concentration of very small ($d_{core} < 4.0$ nm) AuNPs. The UV-vis spectrum of the PAH–AuNP supernatant and a representative TEM image are provided in

the ESI† as Fig. S7. CTAB–AuNR supernatant significantly caused mortality at 50 μg L^{-1}, eliciting 100% mortality in *D. magna* exposures ($U = 0$, $p < 0.05$).

Effects of chronic AuNP exposures on daphnid survival, reproduction, and body size

PAH (positively charged) and Cit–AuNPs (negatively charged) were the only functionalized AuNPs that significantly decreased daphnid reproduction over the 21 day chronic exposure (Fig. 4a and b). PAH–AuNPs significantly decreased reproduction at 5 μg L^{-1} (12% decrease, $U = 10$, $p < 0.05$) (Fig. 4a). In contrast, the free ligand PAH, significantly increased reproduction in daphnids (10% increase, $U = 7$, $p < 0.05$; and 13% increase, $U = 8$, $p < 0.05$) at both 1 μg L^{-1} and 5 μg L^{-1} concentrations. Daphnid exposed to the CTAB free ligand also experienced increased reproduction by 20% in 5 μg L^{-1} exposures ($U = 3$, $p < 0.05$) but the CTAB supernatant decreased reproduction by 18% at 1 μg L^{-1} ($U = 9.5$, $p < 0.05$). For negatively charged particles, Cit–AuNPs significantly decreased daphnid reproduction (97% decrease, $U = 0$, $p < 0.05$) at 25 mg L^{-1} averaging only 3 *D. magna* neonates per individual compared

This journal is © The Royal Society of Chemistry 2014

*Environ. Sci.: Nano*, 2014, **1**, 260–270 | **265**
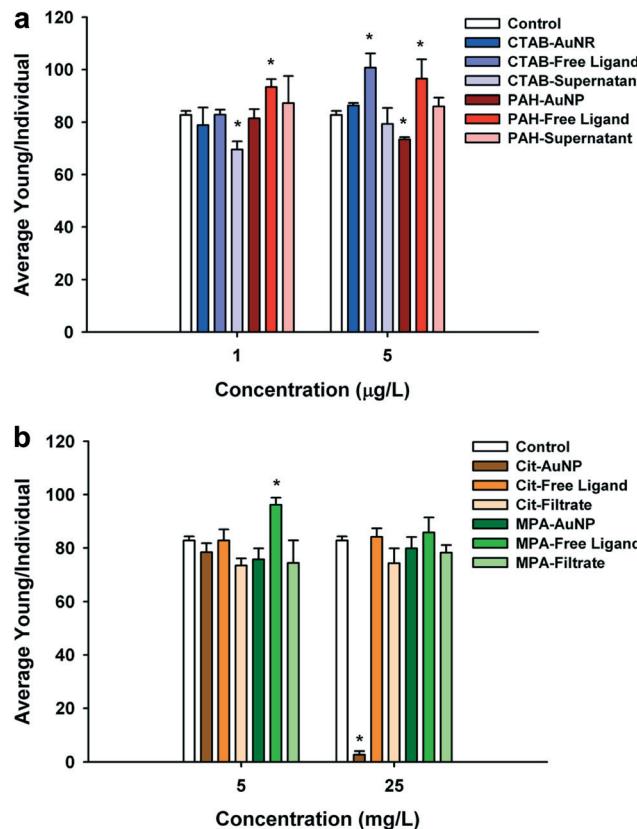
Fig. 4 Effects of AuNPs, free ligands and impurities on daphnid reproduction in chronic assays. Effects of AuNP exposure on (a) daphnid reproduction after 21 day exposure to 1 and 5 μg L^{-1} CTAB or PAH–AuNPs, free ligands and supernatants and (b) daphnid reproduction after 21 day exposure to 5 and 25 mg L^{-1} Cit or MPA–AuNPs, free ligands and filtrates. Reproduction evaluated by Mann–Whitney U test for two independent samples. Asterix indicate significant difference from control ($p < 0.05$).

to 83 neonates per individual control daphnids (Fig. 4b). MPA–AuNPs had no impact yet at 5 mg L^{-1} the MPA free ligand increased reproduction by 14% ($U = 4$, $p < 0.05$).

Daphnia magna exposed to 25 mg L^{-1} Cit–AuNPs and MPA–AuNPs exhibited a significant reduction in adult body size as compared to control daphnids ($U = 0$, $p < 0.05$; and $U = 0$, $p < 0.05$) (Fig. 5), while daphnids exposed to CTAB and PAH showed no significant reduction in daphnid body size. At 25 mg L^{-1}, Cit–AuNPs reduced daphnid growth by 15% compared to control daphnids, having an average length of 3.36 mm compared to 3.85 mm, respectively and exposure to MPA–AuNPs elicited a 7% reduction in daphnid body size, averaging 3.57 mm body length. Since chronic exposures were conducted at sub lethal levels as determined by acute exposures we did not observe any significant mortality for any of the chronic NP exposures.

Effects of surface chemistry on AuNP uptake in *Daphnia magna*

The surface chemistry of the AuNPs was found to have minimal influence on NP uptake by daphnids in this study (Fig. S6†), as ICP-MS analysis indicated that all the AuNPs tested were found to be taken up by daphnids in similar amounts (on a
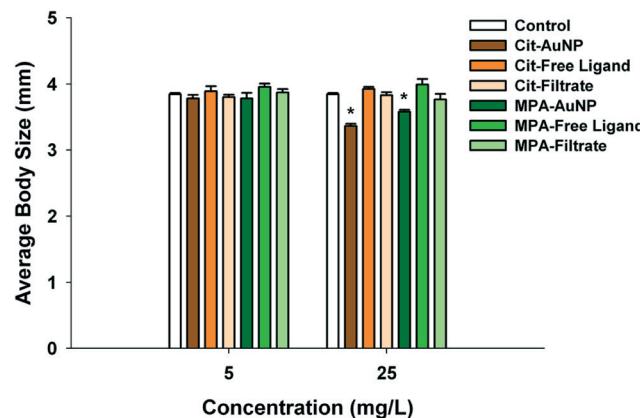
Fig. 5 Effects of AuNPs on daphnid body size after 21 day chronic exposure. Effects of AuNP exposure on daphnid body size after 21 day exposure to 5 and 25 mg L^{-1} of Cit or MPA AuNPs. Body size evaluated by Mann–Whitney U test for two independent samples. Asterix indicate significant difference from control ($p < 0.05$).

per mass basis). However, MPA–AuNPs were significantly taken up ($p < 0.05$) to a greater extent when compared to PAH–AuNPs and Cit–AuNPs even though it is still relatively comparable throughout treatments. Additionally, there was no significant difference in the quantity of NPs on the daphnid carapace and minimal accumulation across all treatments when iodide treated samples were compared to samples without the iodide treatment.

Discussion

Initial particle charge significantly impacted overall toxicity observed in this study, with positively-charged particles being more toxic than their negatively-charged counterparts. Positively-charged particles, PAH and CTAB–AuNPs, were orders of magnitude more toxic than negatively-charged citrate and MPA–AuNPs, significantly eliciting mortality in *Daphnia magna* down to a concentration of 10 μg L^{-1}. In addition, PAH–AuNPs significantly affected daphnid reproduction at 5 μg L^{-1} whereas Cit–AuNPs affected *Daphnia magna* reproduction at 25 mg L^{-1} (Fig. 4a and b). Toxicity caused by imparting positive charge to NPs has been shown with other cells, mammals and aquatic organisms such as algae, bivalves and fish.[7,10,64–67] One study in particular, demonstrated a charge dependent response when exposing zebrafish to AuNPs. When 0.8 nm and 1.5 nm AuNPs functionalized with a cationic surface group, trimethylammoniumethanethiol (TMAT), were more toxic than anionic 2-mercaptoethanesulfonate (MES) or neutral charged 2-(2-mercaptoethoxy)ethanol (MEE) surface groups, affecting mortality, morphology, behavior and developmental endpoints to a greater extent.[65]

One possible reason that PAH and CTAB–AuNPs were more toxic than their negatively-charged counterparts is potentially due to these particles having a high affinity towards the nega-tive charged surfaces of cellular membranes.[68] The high level of attraction that positive charged particles have with cellular membranes increases cellular uptake of these particles through

266 | *Environ. Sci.: Nano*, 2014, **1**, 260–270

This journal is © The Royal Society of Chemistry 2014

mechanisms such as phagocytosis, pinocytosis and membrane disruption, which creates holes in the membrane due to the densely populated charge on the NP surface.[69,70] This allows the positive charged particles to enter the intracellular matrix and potentially damage cell organelles integral to cellular functions. Lovern *et al.* (2008)[71] and García-Cambero *et al.* (2013)[72] observed the uptake of gold NPs *in vivo* with minimal evidence of AuNPs ability to cross the *Daphnia magna* digestive tract. However, these studies were not focused on positively-charged particles, which have a greater potential to be further incorporated into the organism. The lack of tissue accumulation of negatively-charged NPs could be one of the potential mechanisms that caused the positively charged NPs to be more toxic and could explain the low toxicity observed with the negatively charged particles.

Another potential explanation for the difference seen in toxicity between the differentially charged particles in our experiment may be due to particle stability and aggregation in our media (MHRW). Positively charged particles, PAH and CTAB–AuNPs, did not aggregate significantly in the media (as can be seen in the UV-vis spectra of these AuNPs, provided in the ESI,† Fig. S3), while negatively charged particles, MPA and Cit–AuNPs, underwent greater aggregation during our experiments (Table 2). Stable particles, PAH–AuNP and CTAB–AuNP, remained less than 100 nm in size (55.9 ± 4.1 and 17.5 ± 0.2, respectively) and the unstable particles, MPA–AuNP and Cit–AuNP, aggregated or agglomerated to a large extent, drastically increasing their size over the period between media exchanges (750.6 ± 8.2 and 90.8 ± 5.9, respectively) (see Fig. 6 and S3–S5†). Aggregation-dependent toxicity has been seen in other studies using zebrafish embryos, leading us to believe that aggregation can affect NP toxicity.[73,74] Although daphnids clearly ingested all functionalized particles (Fig. S6†) the aggregation size may cause a difference in their interactions with daphnid, potentially affecting the surface area of the particle available for interaction with the cells within the organism, as well as the potential uptake into cells.

The smaller size of the positively-charged particles in our study may have increased their toxicity by enabling them to cross the gut lumen of the daphnids, potentially further interacting with *D. magna* cells and organelles vital to daphnid homeostasis and other functions. This could account for the high mortality seen at low concentrations, especially because the PAH–AuNP supernatant exposure produced high mortality and TEM images revealed a small amount of <4 nm PAH–AuNPs present in the supernatant suspension (Fig. S7†). Small, 10 nm positively-charged amine coated AuNPs have been shown to enter a freshwater bivalve's branchial and digestive epithelial cells, entering the cytoplasm where the particles were then able to penetrate the cells nucleus and lysosomial vesicles.[64] AuNPs with core diameters less than 50 nm (15 and 50 nm AuNPs) have also been shown to affect inner organs of rats to a greater extent than larger particles (160 nm).[24,75] Similar size dependent toxicity has been shown in aquatic organisms with various NP types.[17] Negatively-charged particles aggregating to a large size have
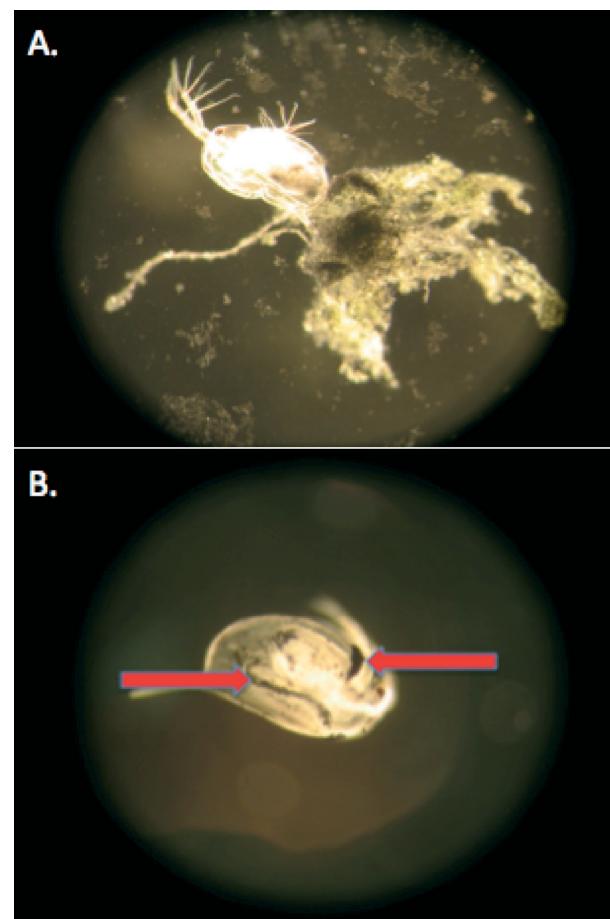

Fig. 6 Nanoparticles adhered to daphnid exoskeleton. Cit–AuNPs adhered to a daphnid carapace. (a) Cit–AuNP algal-agglomerate adhering to daphnid carapace. (b) Cit–AuNPs are ingested by daphnids but may also be found on the outside of the daphnids.

fewer mechanisms to enter the cell, reducing the ability to cross the cellular membrane and damage cell organelles. Main routes of entry of larger particles are through macropinocytosis, phagocytosis and clathrin mediated endocytosis.[69] Other studies have shown that larger particles and aggregates are less toxic than their smaller, monodispersed counterparts.[21,32,34] For example, increasing the extent of aggregation therefore increasing the particle size of MPA–AuNPs, reduced their toxicity to zebrafish embryos.[73,74]

MPA and Cit–AuNPs did impact reproduction (at high concentrations of Cit–AuNP, Fig. 4b) and body size (Fig. 5), however we observed unusual aggregation in the chronic exposures for these two particles. Cit–AuNPs, the more toxic of the two negatively-charged particles, formed agglomerates as appose to aggregates (Fig. 2). These agglomerates could not be re-suspended and formed a film on the bottom of the beaker. TEM imaging of the AuNP aggregates confirms that the Cit–AuNPs form extended wires and larger spherical AuNPs as a result of their aggregation process as appose to the MPA–AuNPs, which remain ~4.0 nm particles, but form large networks of closely associated AuNPs. We hypothesize that these agglomerates could cause an impact on the energy

This journal is © The Royal Society of Chemistry 2014

Environ. Sci.: Nano, 2014, **1**, 260–270 | **267**

budgets of these organisms either through blocked nutrient absorption or a decrease in food consumption[76] or due to an impact on swimming and molting as these particles were found to adhere to the exoskeleton, adding mass to the swimming organism (Fig. 6). Lee and Ranville (2012)[77] while conducting a 48 hour acute assay using *D. magna*, found that organisms exposed to aggregated Cit–AuNPs shed their exoskeletons while the controls did not. The increased molting observed in the Cit–AuNP exposed daphnids demonstrates that *Daphnia magna* may use this tactic to avoid any unwanted effects caused by the adhered Cit–AuNPs, however, the increased molting requires energy, leaving less for daphnid growth and reproduction.

Certain ligands used to alter the surface chemistry of NPs are more toxic than others, which could also explain the increased toxicity of CTAB–AuNRs in particular in our study. For the CTAB ligands, the acute ligand toxicity exactly matched the acute toxicity of the CTAB–AuNR, while the PAH ligand was only toxic when paired with the gold NP (Fig. 3). For CTAB–AuNRs, it is widely accepted that improper purification or ligand desorption can result in free-floating CTAB ligands in NP suspensions, which leads to this functionalized particle being highly toxic.[13] This potentially downplays the effect of charge on toxicity for this functionalized AuNP. However, both ligand concentrations in the particle suspensions were much lower than what we tested in the free ligand control experiments implying that there is another mechanism that causes the ligands as well as the particles to become more toxic. We hypothesize that the increase in PAH and CTAB toxicity when attached to the gold NPs may be due to an increase in the concentration of PAH and CTAB inside the daphnids gut due to their ingestion with the NP and localization of ligand on or in daphnid cells. There were some indications of an increase in the reproduction of daphnids in the presence of the free ligand of CTAB, PAH and MPA. This may be due to some physiological use for the daphnids of these functional groups but may also be due to a hormesis effect of the ligands where a small amount of these chemicals is stimulatory to the organism's biochemical mechanisms that deal with toxins and therefore an up-regulation of other pathways dealing with reproduction. This may be a life history strategy for the organism to increase reproduction in a time of stress, as seen by others.[78,79]

Lastly, in this experiment, the effects of ligand density and gold dissolution on NP toxicity are thought to be minimal. The similarity in ligand densities determined by XPS results (Table 3) for these ligands demonstrates that the differences in subsequent biological interaction are not likely to be associated with differences in ligand density. Additionally, it should be noted that while functionalized AuNPs may be susceptible to aggregation under specific environmental conditions, AuNPs are not readily susceptible to dissolution or oxidation under typical environmental conditions (which is in contrast to many functionalized silver or metal oxide NPs).[38–41] As a consequence, when we considered how AuNP stability influences toxicity in this discussion, we focused primarily on the stability of AuNPs against aggregation, rather than dissolution or oxidation.

The results of this study are important, because it identifies mechanisms for AuNP toxicity by examining NP toxicity with different charges using an environmentally relevant organism. The present study and our previous work[23] demonstrate the need for functionalized NPs to be evaluated in chronic exposures, as acute exposures do not explain the full adverse affects of NPs on aquatic organisms, as seen with Cit–AuNPs. This study also demonstrates that characterization of NP size after exposure to media as well as accounting for free ligand and synthesis impurity toxicity are important in determining the mechanism for NP toxicity.

Conclusion

NPs have the potential to be highly beneficial to society, however in order to create NPs that are beneficial, while minimizing the environmental implications of these materials, the mechanisms that govern the toxicity of NPs need to be better elucidated. We found that surface chemistry plays a significant role in NP toxicity; not only does the charge of the ligand on the AuNP surface influence both acute and chronic toxicity, but the identity of the ligand itself can influence toxicity. Interestingly, ~4.0 nm AuNPs functionalized with a non-toxic ligand (PAH) showed significant acute and chronic toxicity. In addition, the smallest particles (<4 nm) as seen in the PAH–AuNP supernatant exposures, could potentially be much more harmful to *Daphnia magna* than comparatively larger sized PAH–AuNPs (>4 nm). Furthermore, the chronic toxicity assays performed in this study indicate that AuNPs that show minimal acute toxicity can induce significant long-term effects, impacting daphnid reproduction. Therefore, chronic toxicity studies are essential for elucidating potential long-term exposures of manufactured NPs. Testing libraries of NPs with a variety of surface chemistries with different effective charges and functionalities in a given study will help discover trends in NP toxicity and translate these experiments to predictions for other types of NPs.

Acknowledgements

References

1 R. J. Aitken, M. Q. Chaudhry, A. B. A. Boxall and M. Hull, *Occup. Med.*, 2006, **56**, 300–306.

2 A. A. Keller, S. McFerran, A. Lazareva and S. Suh, *J. Nanopart. Res.*, 2013, **15**, 1692–1708.

3 E. V. Rogozhina, D. A. Eckhoff, E. Gratton and P. V. Braun, *J. Mater. Chem.*, 2006, **16**, 1421–1430.

4 B. G. Trewyn, I. I. Slowing, S. Giri, H. T. Chen and V. S. Y. Lin, *Acc. Chem. Res.*, 2007, **40**, 846–853.

5   Y. Zhang, N. Kohler and M. Q. Zhang, *Biomaterials*, 2002, **23**, 1553–1561.

6   R. M. Crist, J. H. Grossman, A. K. Patri, S. T. Stern, M. A. Dobrovolskaia, P. P. Adiseshaiah, J. D. Clogston and S. E. McNeil, *Integr. Biol.*, 2013, **5**, 66–73.

7   C. M. Goodman, C. D. McCusker, T. Yilmaz and V. M. Rotello, *Bioconjugate Chem.*, 2004, **15**, 897–900.

8   N. Lewinski, V. Colvin and R. Drezek, *Small*, 2008, **4**, 26–49.

9   Z.-J. Zhu, R. Carboni, M. J. Quercio, B. Yan, O. R. Miranda, D. L. Anderton, K. F. Arcaro, V. M. Rotello and R. W. Vachet, *Small*, 2010, **6**, 2261–2265.

10 A. M. El Badawy, R. G. Silva, B. Morris, K. G. Scheckel, M. T. Suidan and T. M. Tolaymat, *Environ. Sci. Technol.*, 2010, **45**, 283–287.

11 K. Isoda, T. Hasezaki, M. Kondoh, Y. Tsutsumi and K. Yagi, *Die Pharmazie - An International Journal of Pharmaceutical Sciences*, 2011, **66**, 278–281.

12 K. L. Aillon, Y. Xie, N. El-Gendy, C. J. Berkland and M. L. Forrest, *Adv. Drug Delivery Rev.*, 2009, **61**, 457–466.

13 A. M. Alkilany, P. K. Nagaria, C. R. Hexel, T. J. Shaw, C. J. Murphy and M. D. Wyatt, *Small*, 2009, **5**, 701–708.

14 D. P. Stankus, S. E. Lohse, J. E. Hutchison and J. A. Nason, *Environ. Sci. Technol.*, 2011, **45**, 3238–3244.

15 M. P. Monopoli, D. Walczyk, A. Campbell, G. Elia, I. Lynch, F. Baldelli Bombelli and K. A. Dawson, *J. Am. Chem. Soc.*, 2011, **133**, 2525–2534.

16 I. Lynch and K. A. Dawson, *Nano Today*, 2008, **3**, 40–47.

17 O. Bar-Ilan, R. M. Albrecht, V. E. Fako and D. Y. Furgeson, *Small*, 2009, **5**, 1897–1910.

18 C. Grabinski, N. Schaeublin, A. Wijaya, H. D'Couto, S. H. Baxamusa, K. Hamad-Schifferli and S. M. Hussain, *ACS Nano*, 2011, **5**, 2870–2879.

19 R. J. Griffitt, L. Jing, G. Jie, J.-C. Bonzongo and D. S. Barber, *Environ. Toxicol. Chem.*, 2008, **27**, 1972–1978.

20 Y. Pan, S. Neuss, A. Leifert, M. Fischler, F. Wen, U. Simon, G. Schmid, W. Brandau and W. Jahnen-Dechent, *Small*, 2007, **3**, 1941–1949.

21 Y. S. Chen, Y. C. Hung, I. Liau and G. S. Huang, *Nanoscale Res. Lett.*, 2009, **4**, 858–864.

22 R. Klaper, J. Crago, J. Barr, D. Arndt, K. Setyowati and J. Chen, *Environ. Pollut.*, 2009, **157**, 1152–1156.

23 D. A. Arndt, M. Moua, J. Chen and R. Klaper, *Environ. Sci. Technol.*, 2013, **47**, 9444–9452.

24 G. S. Terentyuk, G. N. Maslyakova, L. V. Suleymanova, B. N. Khlebtsov, B. Y. Kogan, G. G. Akchurin, A. V. Shantrocha, I. L. Maksimova, N. G. Khlebtsov and V. V. Tuchin, *J. Biophotonics*, 2009, **2**, 292–302.

25 J. F. Hillyer and R. M. Albrecht, *J. Pharm. Sci.*, 2001, **90**, 1927–1936.

26 K. Yin Win and S.-S. Feng, *Biomaterials*, 2005, **26**, 2713–2722.

27 C. Foged, B. Brodin, S. Frokjaer and A. Sundblad, *Int. J. Pharm.*, 2005, **298**, 315–322.

28 M. S. Cartiera, K. M. Johnson, V. Rajendran, M. J. Caplan and W. M. Saltzman, *Biomaterials*, 2009, **30**, 2790–2798.

29 O. F. Karatas, E. Sezgin, O. Aydin and M. Culha, *Colloids Surf., B*, 2009, **71**, 315–318.

30 A. Albanese, P. S. Tang and W. C. W. Chan, *Annu. Rev. Biomed. Eng.*, 2012, **14**, 1–16.

31 A. E. Nel, L. Mädler, D. Velegol, T. Xia, E. M. V. Hoek, P. Somasundaran, F. Klaessig, V. Castranova and M. Thompson, *Nat. Mater.*, 2009, **8**, 543–557.

32 L. Truong, T. Zaikova, E. K. Richman, J. E. Hutchison and R. L. Tanguay, *Nanotoxicology*, 2012, **6**, 691–699.

33 A. Albanese and W. C. W. Chan, *ACS Nano*, 2011, **5**, 5478–5489.

34 S. B. Lovern and R. Klaper, *Environ. Toxicol. Chem.*, 2006, **25**, 1132–1137.

35 A. M. Alkilany and C. J. Murphy, an interdisciplinary forum for nanoscale science and technology, *J. Nanopart. Res.*, 2010, **12**, 2313–2333.

36 A. Ostrowski, T. Martin, J. Conti, I. Hurt and B. Harthorn, *J. Nanopart. Res.*, 2009, **11**, 251–257.

37 A. Kroll, M. H. Pillukat, D. Hahn and J. Schnekenburger, *Eur. J. Pharm. Biopharm.*, 2009, **72**, 370–377.

38 C. J. Murphy, A. M. Gole, J. W. Stone, P. N. Sisco, A. M. Alkilany, E. C. Goldsmith and S. C. Baxter, *Acc. Chem. Res.*, 2008, **41**, 1721–1730.

39 K. Kenison Falkner and J. M. Edmond, *Earth Planet. Sci. Lett.*, 1990, **98**, 208–221.

40 K. B. Krauskopf, *Econ. Geol. Bull. Soc. Econ. Geol.*, 1951, **46**, 858–870.

41 A. M. Alkilany, S. E. Lohse and C. J. Murphy, *Acc. Chem. Res.*, 2012, **46**, 650–661.

42 J. Aaron, E. de la Rosa, K. Travis, N. Harrison, J. Burt, M. JosÈ-Yacam·n and K. Sokolov, *Opt. Express*, 2008, **16**, 2153–2167.

43 N. Calander, *Curr. Anal. Chem.*, 2006, **2**, 203–211.

44 G. F. Paciotti, L. Myer, D. Weinreich, D. Goia, N. Pavel, R. E. McLaughlin and L. Tamarkin, *Drug Delivery*, 2004, **11**, 169–183.

45 D. Pissuwan, T. Niidome and M. B. Cortie, *J. Controlled Release*, 2011, **149**, 65–71.

46 C. Corti and R. Holliday, *Gold Bull.*, 2004, **37**, 20–26.

47 N. Khlebtsov and L. Dykman, *Chem. Soc. Rev.*, 2011, **40**, 1647–1671.

48 S. E. Lohse, J. R. Eller, S. T. Sivapalan, M. R. Plews and C. J. Murphy, *ACS Nano*, 2013, **7**, 4135–4150.

49 N. R. Jana, L. Gearheart and C. J. Murphy, *Langmuir*, 2001, **17**, 6782–6786.

50 S. F. Sweeney, G. H. Woehrle and J. E. Hutchison, *J. Am. Chem. Soc.*, 2006, **128**, 3190–3197.

51 A. Gole and C. J. Murphy, *Chem. Mater.*, 2004, **16**, 3633–3640.

52 C. J. Ackerson, P. D. Jadzinsky and R. D. Kornberg, *J. Am. Chem. Soc.*, 2005, **127**, 6550–6551.

53 T. K. Sau and C. J. Murphy, *Langmuir*, 2004, **20**, 6414–6420.

54 G. H. Woehrle, J. E. Hutchison, S. Özkar and R. G. Finke, *Turk. J. Chem.*, 2006, **30**, 1–13.

55 J. W. McMahon and F. H. Rigler, *Limnol. Oceanogr.*, 1965, **10**, 105–113.

56 EPA, *Standard operating procedure for moderately hard reconstituted water*, SoBran, Dayton, OH, USA, 2003.

57 U. S. E. P. Agency, in *SoBran*, Dayton, OH, USA, 2003.

This journal is © The Royal Society of Chemistry 2014

Environ. Sci.: Nano, 2014, **1**, 260–270 | 269

58 W. Haiss, N. T. K. Thanh, J. Aveyard and D. G. Fernig, *Anal. Chem.*, 2007, **79**, 4215–4221.

59 C. J. Orendorff and C. J. Murphy, *J. Phys. Chem. B*, 2006, **110**, 3990–3994.

60 OECD. *Guidelines for testing of chemicals*, 211, OECD/OCDE, Washington, DC, 1998, 1–21.

61 W. P. Wuelfing, S. M. Gross, D. T. Miles and R. W. Murray, *J. Am. Chem. Soc.*, 1998, **120**, 12696–12697.

62 C. J. Orendorff, T. M. Alam, D. Y. Sasaki, B. C. Bunker and J. A. Voigt, *ACS Nano*, 2009, **3**, 971–983.

63 B. Nikoobakht and M. A. El-Sayed, *Langmuir*, 2001, **17**, 6368–6374.

64 S. Renault, M. Baudrimont, N. Mesmer-Dudons, P. Gonzalez, S. Mornet and A. Brisson, *Gold Bull.*, 2008, **41**, 116–126.

65 S. Harper, C. Usenko, J. E. Hutchison, B. L. S. Maddux and R. L. Tanguay, *J. Exp. Nanosci.*, 2008, **3**, 195–206.

66 A. Asati, S. Santra, C. Kaittanis and J. M. Perez, *ACS Nano*, 2010, **4**, 5321–5331.

67 Y. Yang, J. Wang, H. Zhu, V. L. Colvin and P. J. Alvarez, *Environ. Sci. Technol.*, 2012, **46**, 3433–3441.

68 E. C. Cho, J. Xie, P. A. Wurm and Y. Xia, *Nano Lett.*, 2009, **9**, 1080–1084.

69 S. D. Conner and S. L. Schmid, *Nature*, 2003, **422**, 37.

70 A. Verma and F. Stellacci, *Small*, 2010, **6**, 12–21.

71 S. B. Lovern, H. A. Owen and R. Klaper, *Nanotoxicology*, 2008, **2**, 43–48.

72 J. P. García-Cambero, M. Núñez García, G. D. López, A. L. Herranz, L. Cuevas, E. Pérez-Pastrana, J. S. Cuadal, M. R. Castelltort and A. C. Calvo, *Chemosphere*, 2013, **93**, 1194–1200.

73 E. Ying and H.-M. Hwang, *Sci. Total Environ.*, 2010, **408**, 4475–4481.

74 M. W. Katrina, M. M. Lisa, C. Z. Richard, J. T. Barbara, J. K. Norman, D. Q. Ryan, B. Somnath, G. T. Justin, G. P. Joel and D. T. Brian, *Toxicol. Sci.*, 2009, **107**, 553–553.

75 W. H. De Jong, W. I. Hagens, P. Krystek, M. C. Burger, A. J. A. M. Sips and R. E. Geertsma, *Biomaterials*, 2008, **29**, 1912–1919.

76 D. Ebert, *National Center for Biotech. Info.*, USA, 2005, Chapter 2.

77 B.-T. Lee and J. F. Ranville, *J. Hazard. Mater.*, 2012, **213–214**, 434–439.

78 C. M. Flaherty and S. I. Dodson, *Chemosphere*, 2005, **61**, 200–207.

79 M. Knops, R. Altenburger and H. Segner, *Aquat. Toxicol.*, 2001, **53**, 79–90.